Highly Enhancing Fluorescence in Microarrays via Tunable Nanostructured Biochips

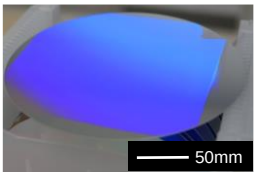

Introduction

Fluorescence based detection serves as a very effective means to identify and detect literally any biomolecule of interest. Often, however, low concentrations can be difficult to detect due to low signal to noise ratios (SNRs). By incorporating metallic nanostructures, which provide highly focused and enhanced optical fields, one can boost the SNR by several orders of magnitude, thereby resulting in highly enhanced fluorescence[1-4]. Building on years of expertise, Moxtek has developed cost effective and reliable methods to obtain uniform wafer scale metallic nanostructured biochips[5-9]. This whitepaper presents their use as fluorescence enhancing substrates for Cy3 based protein microarrays. We are ready to support your needs, from developmental projects through commercialization.

Method/NHA Effect (Fabrication)

By take advantage of the plasmonic effects offered by aluminum nanohole arrays (Al NHAs), we are able to obtain substrates for fluorescence based detection that can offer more than an order of magnitude increase of the SNR. Whole 200mm diameter glass wafers coated with a thin film of aluminum are patterned with a periodic NHA pattern. The result, seen in fig. 1, is a very well defined hole morphology and clear repetition both on the nanoscale and the wafer scale. Moreover, the Al NHA, designed to enhance the fluorescence of the dye Cy3, shows a transmission peak centered right at 532nm (fig. 2), which is the most common laser excitation wavelength used for this fluorophore. This transmission peak is indicative of the plasmonic resonance that is supported by this structure at this wavelength. The resonance can also be clearly visualized in fig. 2 where we have plotted the magnitude of the electric field at 532nm, both at a cross section along the base of a nanohole and along its height as well (modeled with Lumerical). These field profile plots (normalized to the magnitude of the incident light) show a strong confinement and increase of light intensity at the base of the nanoholes. It is specifically at the base of the nanoholes where biomolecules will be immobilized.

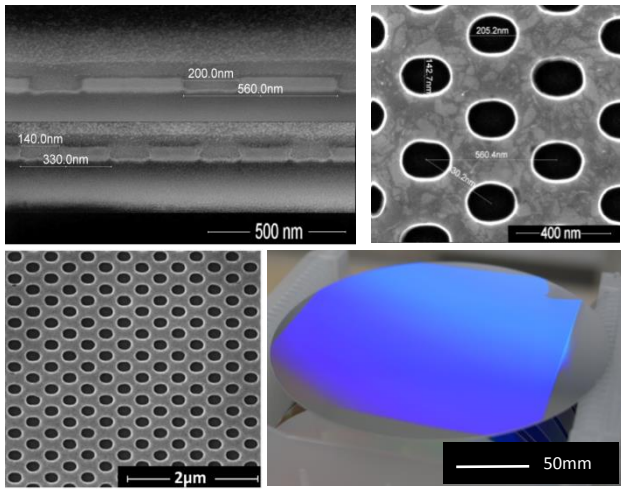

Fig. 1. SEM cross sectional and top view images of the full 200mm wafer patterned Al NHA.

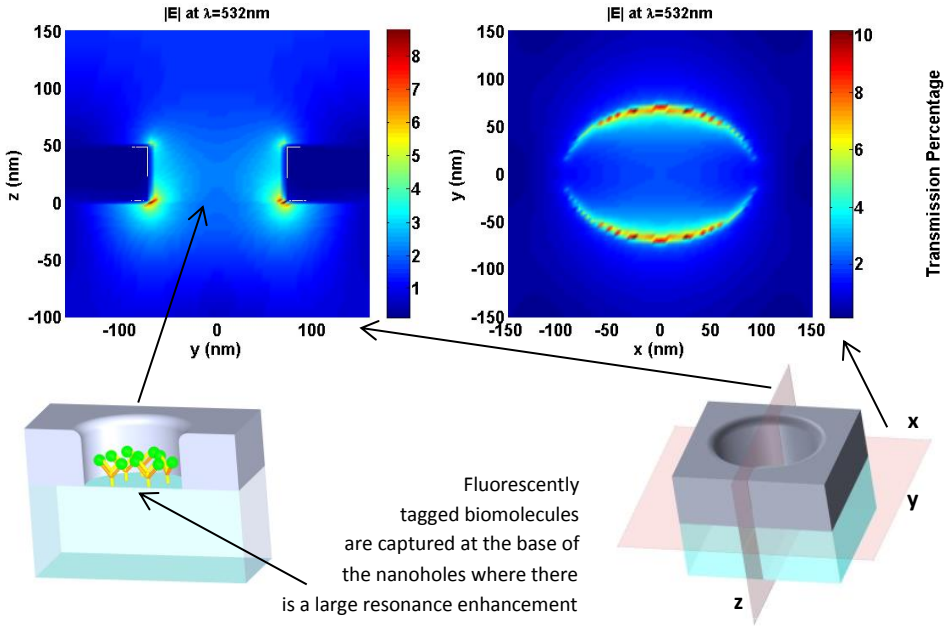

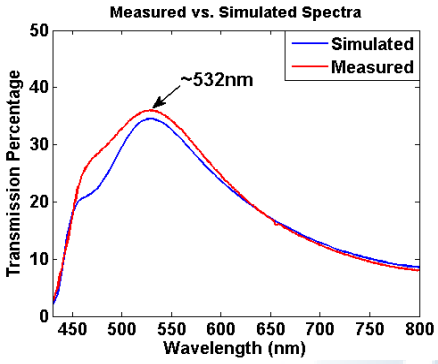

Fig. 2. Simulated and measured optical transmission of the Al NHA designed for the fluorescence enhancement of Cy3 along with corresponding electric field profile plots at the laser excitation λ=532nm.

Substrate Preparation and Experimental Design

Standard 25x75mm slides are cut from the 200mm Al NHA patterned glass wafers. The substrates are then thoroughly cleaned in methanol, IPA, and then an ultrasonic DI water bath to remove any possible contaminants. The Al surface of the nanoholes is then passivated with a protective coating (Moxtek proprietary) and the slides are functionalized with a standard epoxysilane. This results in a structure which only allows for binding of biomolecules at the glass base of the nanoholes where the plasmonic hot spots reside (figs. 2 and 3).

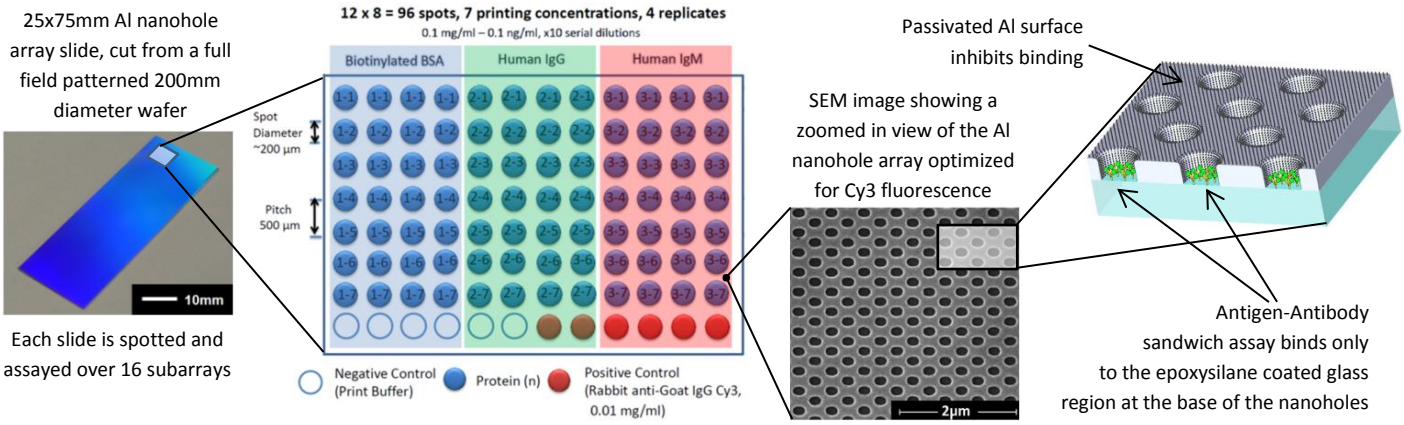

Fig. 3. Schematic outline depicting the microarray based spotting and binding of biomolecules on the Al NHA slides.

In order to evaluate the fluorescence sensing capabilities of the Al NHAs, a series of standard fluorescence based microarray tests were carried out. Various slides were each spotted with 4 duplicates of the three antigens Human IgG, IgM, and biotinylated BSA at concentrations of 0.1mg/ml – 0.1ng/ml over x10 serial dilutions (fig. 3). Additional positive and negative control spots were also added. This was repeated over 16 subarrays. The subarrays were then assayed with the corresponding Cy3 labeled antibodies of Human IgG, IgM, and Streptavidin at a concentration of 0.1ug/ml. This process was carried out on the passivated Al NHA slide functionalized with epoxysilane and also on two commercial standards: Schott Nexterion E and HiSens E slides (both of which come with an optimized epoxysilane coating), used as baselines for comparison. Each of the three assays was carried out over multiple subarrays within the 16 subarray set, and the results from multiple spots over the multiple subarrays were then averaged in order to yield a meaningful standard for comparison between the different slides.

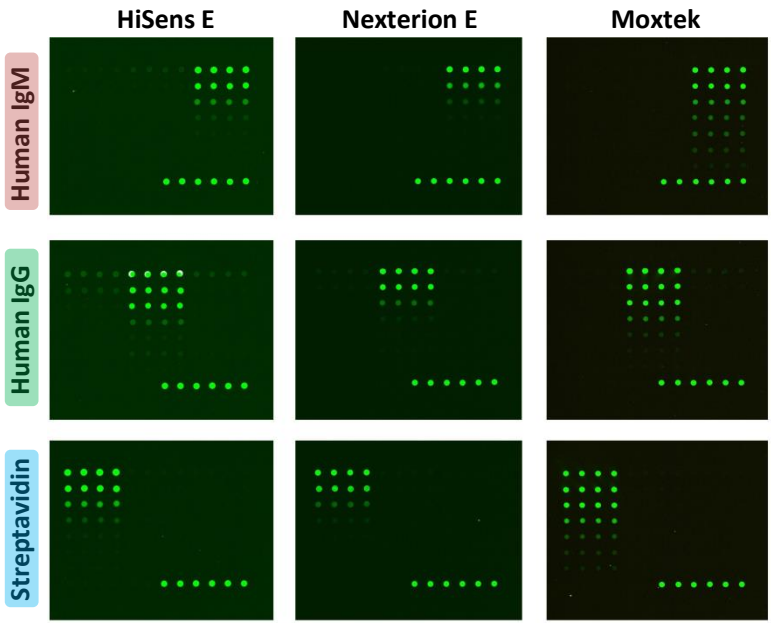

Fig. 4. Side by side comparisons of the fluorescence results on the Moxtek slide and the two Schott standards for all 3 tested assays.

Experimental Fluorescence Results

As seen in the side by side comparison (fig. 4), the Moxtek slide shows a very pronounced enhancement of the fluorescence, especially at the lowest concentrations, while maintaining the same low background levels as the Nexterion slide (HiSens slide has a ~3x higher background). This allows for detection of even the lowest printed antigen concentrations. In

comparison, on the Nexterion and the HiSens slides, the three lowest and two lowest concentrations are undetectable (fig. 5). Furthermore, up to 25x and 11x enhancements of the fluorescence SNR are seen in comparison to the Nexterion and HiSens slides respectively (fig. 5). Note that the Moxtek slide may even show a higher enhancement at the lowest concentration, however, such a comparison cannot be properly made, simply because at these concentrations the fluorescence of the other slides falls below their background. At such concentrations where a fluorescence signal was undetectable, the SNR was assumed to be unity, simply in order to obtain some sort quantitative comparison.

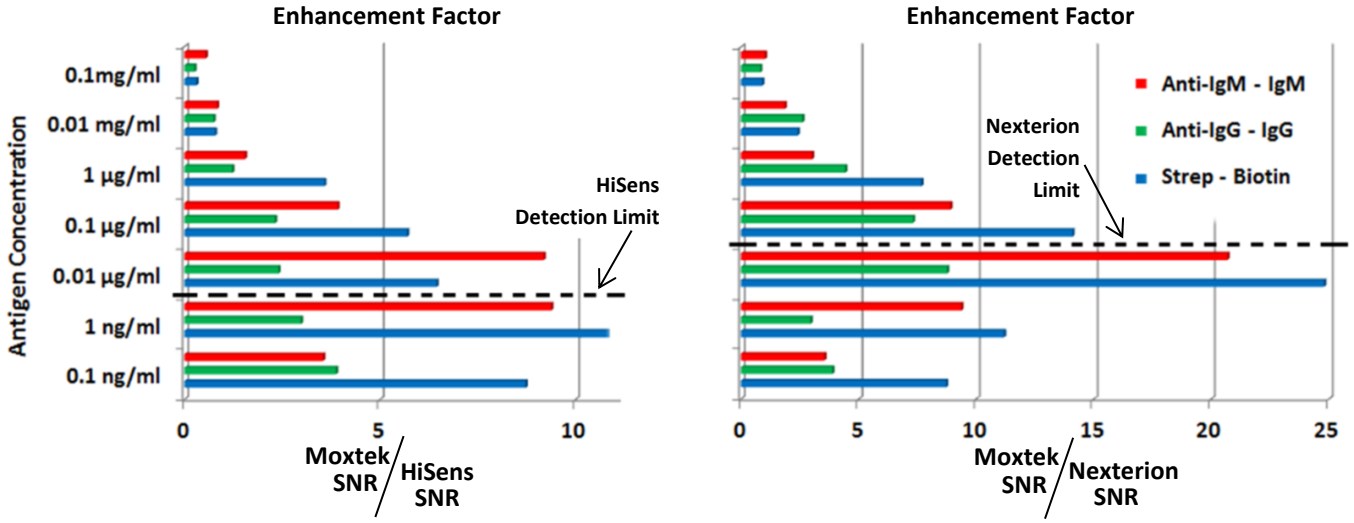

Fig. 5. Comparisons of the fluorescence SNR on the Moxtek Al NHA slide versus that on the two Schott standards Nexterion E and HiSens E. The shown enhancement factor is calculated as the ratio of the experimentally measured fluorescence SNR at each spotting concentration between the two slides being compared. The Moxtek slide shows a very distinct advantage as the spotted antigen concentration is reduced. Fluorescence SNR is calculated as (total fluorescence - background fluorescence)/(background standard deviation).

In order to verify that the binding of the biomolecules is occurring at the base of the nanoholes and that it is indeed the plasmonic resonance of the nanohole array that is providing this observed fluorescence enhancement, we display in fig. 6 the fluorescence images of the 0.1ug/ml Streptavidin-Biotin assay from the Moxtek Al NHA slide and 3 additional control slides: a plain Moxtek glass slide with only an epoxysilane coating, a planar 10nm Al film slide with the same epoxysilane coating, and a planar 10nm Al film slide with a pre-deposited passivation coating and then the applied epoxysilane coating. The results show that the Moxtek Al NHA slide offers a clear advantage over the Moxtek glass slide as expected. Furthermore, though the planar Al slide with only an epoxysilane coating shows a much lower fluorescence signal than either of the other two slides and also a higher background (because it is highly reflective over the entire visible spectrum), it still shows a very apparent signal in comparison to the passivated and then epoxysilane coated planar Al slide. This demonstrates that the passivation coating indeed blocks the aluminum surface almost entirely and that the binding of the biomolecules must therefore be occurring only at the exposed glass base of the nanoholes.

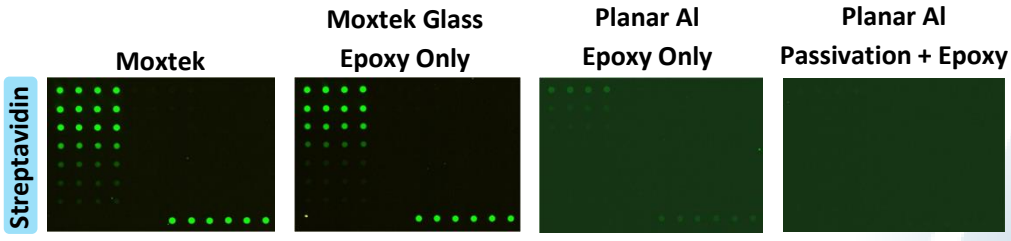

Fig. 6. Comparisons of the imaged fluorescence for the Streptavidin assay on the Moxtek Al NHA slide, a plain Moxtek glass slide with only an epoxysilane coating, a planar 10nm Al film slide with the same epoxysilane coating, and a planar 10nm Al film slide with a pre-deposited passivation coating and then an applied epoxysilane coating.

Conclusions

Standard microarray based fluorescence protocols were carried out on an Al nanohole array (NHA) patterned slide obtained from a fully patterned 200mm diameter glass wafer. The process involved spotting with 4 duplicates of the three antigens Human IgG, IgM, and biotinylated BSA at concentrations of 0.1mg/ml - 0.1ng/ml over x10 serial dilutions. Additional positive and negative control spots were also added and the process was repeated over 16 subarrays on a single slide. The subarrays were then assayed with the corresponding Cy3 labeled antibodies of Human IgG, IgM, and Streptavidin at a concentration of 0.1ug/ml. Fluorescence results were then averaged from multiple spots over multiple subarrays. This process was also carried out on two commercial standards: Schott Nexterion E and HiSens E slides, which served as baseline for comparison. The resulting fluorescence images and quantitative results showed that the Moxtek Al NHA slide offered a very clear advantage, especially as the antigen concentration was decreased. In fact, the Moxtek slide offered at least 11x and 25x enhancements of the fluorescence SNR over the Schott HiSens E and Nexterion E slides respectively at these lower concentrations. Aluminum nanohole array substrates are now available. Please contact Moxtek for additional details.

Summary of Benefits

- (Low Background + Enhanced Fluorescence) = Greater SNR
- Enhanced SNR especially at low concentrations
- Up to 11x+ and 25x+ enhancement over two commercial standards
- Detection over a large dynamic range
- Excellent Specificity
- Clear advantage over the current standards

Other Potential Applications

- Surface enhanced Raman spectroscopy
- Label free detection
- Point of care diagnostics
- Clinical Diagnostics

References

[1] M. Diwekar, S. Attavar, S. Blair, M. Davis, E. Gardner, "Enhanced Fluorescence Sensing with nano-apertures," *Proc. of SPIE* 7604, 760410 (2010) [doi:10.1117/12.845615].

[2] S. Attavar, M. Diwekar, S. Blair, "Photoactivated capture molecule immobilization in plasmonic nanoapertures in the ultraviolet," *Lab Chip* **11,** 841-844 (2011) [doi:10.1039/c0lc00498g]

[3] X. Jiao, E.M. Peterson, J.M. Harris, S. Blair, "UV Fluorescence Lifetime Modification by Aluminum Nanoapertures," *ACS Phot.* **12,** 1270-1277 (2014) [doi:10.1021/ph500267n].

[4] M.I. Stockman, "Nanoplasmonics: past, present, and glimpse into future," *Opt. Express.* **19,** 22029-22106 (2011) [doi:10.1364/OE.19.022029].

[5] M.C. George, S. Nielson, R. Petrova, J. Frasier, E. Gardner, "Wafer-scale aluminum nano-plasmonics," *Proc. of SPIE* 9163, 91633B (2014) [doi:10.1117/12.2062633].

[6] M.C. George, J.-N. Liu, A. Farhang, B. Williamson, M. Black, T. Wangensteen, J. Fraser, R. Petrova, and B.T. Cunningham, "Wafer-scale photonic and plasmonic crystal sensors," *Tech Connect World Innovation Conference and Expo* (2015).

[7] A. Farhang, et al., "Wafer –scale elliptical nanohole arrays," *SPP7 Conference* (2015).

[8] George, M.C., et al., "Wafer-scale Plasmonic and Photonic Crystal Sensors," Proc. SPIE 9547, Metallic Nanostructures and Their Optical Properties XIII, 95471F (2015). doi:10.1117/12.2188631

[9] A. Farhang, et al., "Wafer-scale Aluminum Plasmonics for Fluorescence Based Biodetection," Proc. SPIE 9550, Biosensing and Nanomedicine VIII, 95500U (21 August 2015); doi: 10.1117/12.2186871

Contact Information: Dr. Arash Farhang, Applications Scientist, afarhang@moxtek.com, +1, (801) 717-4250

Moxtek, Inc. 452 W 1260 N, Orem, UT 84057, USA, www.moxtek.com